Bull. Mater. Sci., Vol. 31, No. 6, November 2008, pp. 903–906. © Indian Academy of Sciences.

Apparent activation energy for densification of α-Al_2O_3 powder at constant heating-rate sintering

W Q SHAO, S O CHEN*,†, D LI, H S CAO, Y C ZHANG and S S ZHANG

College of Physics Science, Qingdao University, Qingdao 266071, P.R. China
†Also at Laboratory of Fibre Materials and Modern Textile, Growing Base for State Key Laboratory, Qingdao University, Qingdao 266071, P.R. China

MS received 14 March 2008; revised 9 April 2008

Abstract. **The apparent activation energy for densification is a characteristic quantity that elucidates the fundamental diffusion mechanisms during the sintering process. Based on the Arrhenius theory, the activation energy for densification of α-Al_2O_3 at constant heating-rates sintering has been estimated. Sintering of α-Al_2O_3 powder has been executed by the way of a push rod type dilatometer. It is shown that the apparent activation energy does not have a single value but depends directly on the relative density. The apparent activation energy corresponding to lower relative density was higher than that corresponding to higher relative density. In addition, the value of the evaluated activation energy is different at the same density level when the Arrhenius plot involves different heating rates.**

Keywords. **Apparent activation energy; Arrhenius theory; constant heating-rate sintering; α-Al_2O_3.**

1. Introduction

The alumina ceramic materials find varied technological applications because of their unique combination of physicochemical properties such as hardness, refractory characteristics, resistance to aggressive media, etc. To tailor the microstructure of alumina to the potential application in service, it is necessary to proceed with a meticulous analysis of sintering, where the relative density and the grain size are usually investigated in the function of soak time, soak temperature, heating rate, and green shaping method.

To establish robust sintering conditions, it is also critical to understand what is/are the mechanism(s) controlling grain growth and densification. Ever since the pioneer theoretical models (Kuczynski 1949; Coble 1961) were established, the sintering processes have been intensively studied for more than half a century. One of the main purposes of these studies is to evaluate the activation energy of sintering for distinguishing the controlling mechanisms and determining the rate-limiting species.

Two different types of methods used for the evaluation of the activation energy are (a) isothermal methods, e.g. rate controlled sintering (RCS) method used by Kutty *et al* (2001) and (b) non-isothermal methods, e.g. constant heating-rate method (Young and Cutler 1970). Although most of the sintering models can be used to evaluate the value of the activation energy of sintering, an Arrhenius plot of $\ln(\dot{\varepsilon}T)$ (where $\dot{\varepsilon}$ is the densification rate, T the absolute temperature) versus the reciprocal of the absolute temperature is usually used for the evaluation (Matsui *et al* 2005; Lahiri *et al* 2006).

The method developed by Wang and Raj (1990) for the evaluation of the activation energy at constant heating rates was very easy and fast for calculation purpose. In their method, the equation for the sintering rate is separated into temperature-dependent, grain-size-dependent, and density-dependent quantities. The apparent activation energy (Q) for densification during sintering was determined experimentally using the time, temperature, and density data from the constant heating-rate sintering experiments. The expression of their method is as follows

$$\ln\left(T\dot{T}\frac{\mathrm{d}\rho}{\mathrm{d}T}\right) = -\frac{Q}{RT} + \ln[f(\rho)] + \ln A - n\ln d, \qquad (1)$$

where $\dot{T}$ (= $\mathrm{d}T/\mathrm{d}t$) is the heating rate, R the gas constant, $f(\rho)$ a function only of density, A the material parameter which was insensitive to d, T, or ρ, d the particle size, n the particle size power law, $n = 3$, if the densification rate was controlled by lattice diffusion, and $n = 4$ for grain boundary diffusion.

To determine Q, a mathematical manipulation using natural logs was used to allow (1) to take on the general form of $y = mx + b$. Assuming that particle size is dependent only on sintered density, Q can be determined for a specific sintered density from an Arrhenius plot of $\ln[T^*(\mathrm{d}T/\mathrm{d}t)^*(\mathrm{d}\rho/\mathrm{d}T)]$ vs $1/T$ of the different constant rate

*Author for correspondence (shaouchen@126.com)

sintering data. This formalism has been applied for a long time for the investigation of sintering (Wang and Raj 1991; Sato and Carry 1996; Ewsuk *et al* 2006).

For the evaluation of the apparent activation energy, a series of runs at constant heating rates over a range of heating rates is needed. It was found that (Fang *et al* 2003) the evaluation of the apparent activation energy was influenced by the heating rates (especially the low heating rates). However, little attention was paid to study what and how the low heating rates influenced the apparent activation energy. In addition, the variation trend of the apparent activation energy with the relative density has not been investigated in detail. The objectives of this study were to evaluate the apparent activation energy of α-Al_2O_3 based on non-isothermal sintering containing different heating rates lower than 5°C min^{-1} only, to determine how the heating rates influence the apparent activation energy and to explore how the activation energy of α-Al_2O_3 varies with the relative density.

2. Experimental

For constant heating-rate sintering, α-Al_2O_3 powder (99·9% purity, Dalian Luming Nanometer Material Ltd, Dalian, China) having an average grain size of 350 nm was mixed with 1 wt% adhesion agent, dried, granulated, and screened to –60 mesh. The powder was pressed using a uniaxial pressure and then further consolidated by cold isostatic pressing at 250 MPa to create bars of ~ 5 × 5 × 45 mm. The binder was burned out at 500°C. This resulted in negligible densification but provided green strength and minimized contamination from any adsorbed species in the raw powder. The green density was measured by geometric method. The green density of α-Al_2O_3 powder compacts were 2·08 ± 0·03 g cm^{-3}. The value of 3·98 g cm^{-3} was used as the theoretical density, which was the monocrystal density.

Constant heating-rate sintering was performed in a push rod type dilatometer (Luoyang Anter-Lirr Instrument CO, LTD, RPZ-03P, Luoyang, China) at four imposed heating rates ranging from 0·5–5°C min^{-1}. Much lower heating rates are very time-consuming and difficult to control accurately. The sample was heated at 5°C min^{-1} from room temperature to 900°C (below which temperature no densification could be detected), followed by a controlled heating rate (0·5, 1, 2 and 5°C min^{-1}) to 1600°C, after which the sample was cooled. The temperature interval used in the study was from 900–1640°C.

The length change measurements were made by a linear voltage differential transducer (LVDT) which was maintained at a constant temperature by means of water circulation from a constant temperature bath. The accuracy of the measurement of change in length was within ± 0·1 μm. The temperature was measured using a calibrated thermocouple which is placed directly above the sample.

3. Results and discussion

Figure 1 shows the plot of $\Delta L/L_0$ % vs temperature for α-Al_2O_3 under different heating rates in air atmosphere. It can be seen from the figure that the onset of shrinkage shifted to higher temperatures with increasing heating rates. The shrinkage of the samples at the heating rate of 0·5, 1, 2 and 5°C min^{-1} were 18·2, 17·5, 17·3 and 16·8%, respectively. The $\Delta L/L_0$ values were converted into relative density using the following relation (Kutty *et al* 2002):

$$\rho = \frac{\rho_G}{(1-\Delta L/L_0)^3}\frac{1}{\rho_0}, \tag{2}$$

where ρ is the relative density of the sintered compacts, ρ_G the density of green compacts, ρ_0 the theoretical density, $\Delta L/L_0$ the shrinkage.

The basic experimental data giving the change in density with temperature are shown in figure 2. The curves

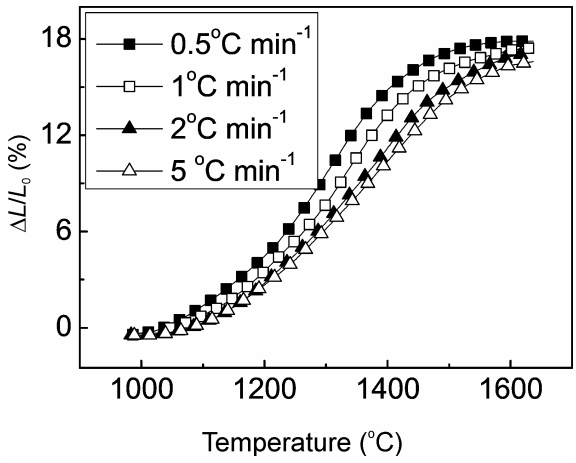

Figure 1. Sintering curves of the α-Al_2O_3 powder compacts at different heating rates.

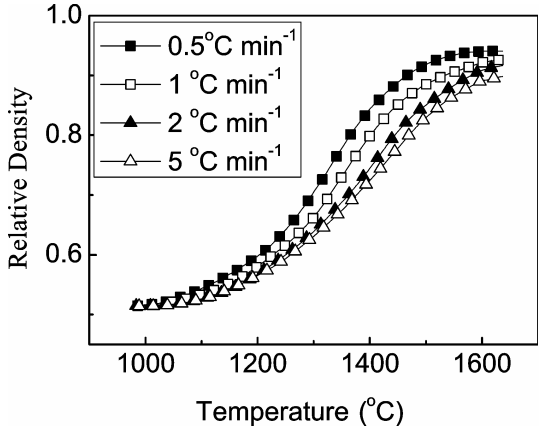

Figure 2. Relative density vs temperature for α-Al_2O_3 powder compacts.

displayed a familiar sigmoidal shape. It can be noted that the sintered densities obtained at any temperature showed a modest but a systematic dependence on heating rates. The maximum density was found to depend upon the heating rate, the higher the heating rate the lower the sintered density. The Archimedes densities of the specimens sintered under 0·5, 1, 2 and 5°C min^{-1} were determined to be 3·79, 3·73, 3·68 and 3·62 g cm^{-3}, respectively.

Non-isothermal dilatometric analyses are commonly reported as shrinkage rate or densification rate vs temperature. Figure 3 shows this type of curve for samples at the heating rate of 0·5–5°C min^{-1}. The instantaneous densification rate increases from green state to the intermediate stage of sintering, undergoes a maximum and then decreases with increasing density. The maximum of the curves shifts slightly to higher temperature with increasing heating rate.

Figure 4 shows the plots of $\ln[T^*(dT/dt)^*(d\rho/dT)]$ vs $1/T$ for different relative densities belonging to the range 0·55–0·89. It is clear that the straight lines obtained are not parallel. Similar phenomena can be found in the literature (Guillaume and Christian 2007). According to the slope of the straight lines, the different apparent values for Q ranging from 678·7 kJ mol^{-1} (0·60 of relative density) to 277·7 kJ mol^{-1} (0·89 of relative density) can be obtained. This interval for the apparent activation energy value includes the traditional 290 (McCoy and Wills 1987)–550 kJ mol^{-1} (Tatami *et al* 2006) (master sintering curve methods) that are reported for pure α-Al_2O_3 material. Compared with the apparent activation energy (0·24 μm α-Al_2O_3, the heating rates were 3, 5, 10, 20°C min^{-1}) value of 739 kJ mol^{-1} (Fang *et al* 2003), the value obtained here was less. The activation energy for sintering is equal to the activation energy for the rate-controlling diffusional mechanism since the sintering rate is proportional to the diffusion coefficient. However, the value obtained for Q can vary drastically, depending on the conditions (i.e. the characteristics of the raw materials, the preparing procedure of green compacts, the sintering procedure, etc) under which the sintering data are obtained. As has been shown in the literature (Fang *et al* 2003), the condition under which the activation energy was obtained differs much more significantly from that in the present work, especially the heating rate (heating rates lower than 5°C min^{-1} only in the present work).

Figure 5 shows that the value of the evaluated activation energy is different at the same density level when the Arrhenius plot involves different heating rates. Like the

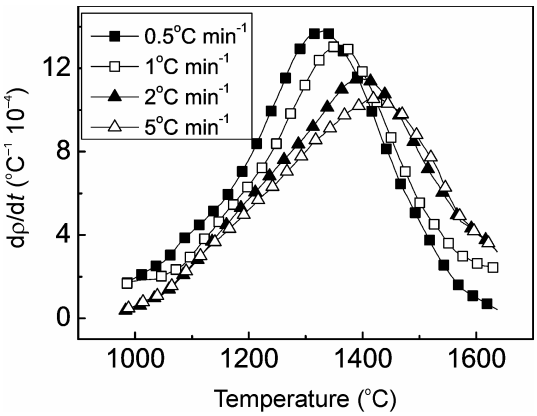

Figure 3. Plots of densification rate and the temperature for α-Al_2O_3 powder compacts.

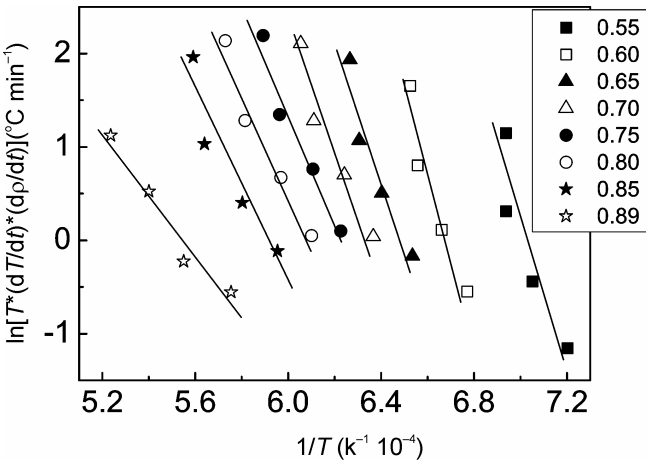

Figure 4. The Arrhenius plot of $\ln[T^*(dT/dt)^*(d\rho/dT)]$ vs $(1/T)$ for the nonisothermal sintering of the powder compacts at different heating rates corresponding to the same relative density.

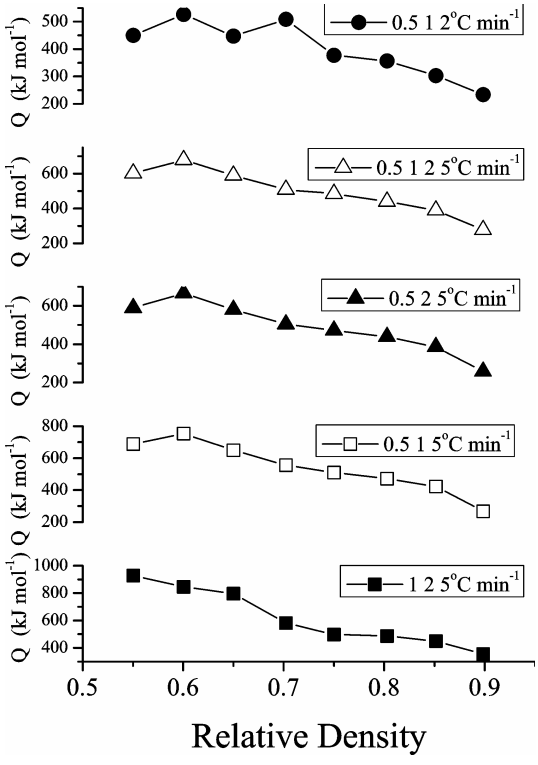

Figure 5. The relative density vs the apparent activation energy calculated based on the Arrhenius plots involving different heating rates.

results obtained above, different activation energy values for 0·21 μm α-Al_2O_3 were evaluated based on different heating rates (Fang *et al* 2003), i.e. 478 kJ mol^{-1} for 10 and 20°C min^{-1}, 640 kJ mol^{-1} for 5, 10, 20°C min^{-1}, and 1080 kJ mol^{-1} for 3, 5, and 10°C min^{-1}, respectively. Based on the MSC theory containing 0·5, 2, 5, 10, 15°C min^{-1}, Su (Su and Johnson 1996) found that the evaluation of activation energy for ZnO was influenced by the lower heating-rate sintering data, i.e. using 0·5–15°C min^{-1}, yields an apparent activation energy of 310 kJ mol^{-1}. Excluding the lowest and the two lowest heating-rate data from the analysis results in estimates of 300 and 285 kJ mol^{-1}, respectively.

According to the sintering theory, the apparent activation energy for densification should be consistent with that of the apparent diffusion coefficient of the rate-limiting species of sintering. In sintering polycrystalline ceramics, it is common that both grain boundary (D_b) and lattice (D_l) diffusion of the rate-limiting species can simultaneously contribute to densification. Because these two diffusivities have different temperature-dependence, the relative contribution of D_l and D_b is different at different temperatures. Thus, heating rate would have a significant influence on the non-isothermal kinetic processes due to the fact that it can change the relative contribution of D_l and D_b from low to high temperatures. Figure 5 indicated that the relative contribution of D_l and D_b to densification for different heating rates is different.

During sintering, surface transport mechanisms (EC, evaporation condensation; SD, surface diffusion) provide for neck growth by moving mass from surface sources. Bulk transport processes (GB, grain boundary diffusion; VD, volume diffusion, PF, plastic flow) provide for neck growth using internal mass sources. Only bulk transport mechanisms cause shrinkage. It is accepted that the GBD or VD are two prominent mechanisms for densification in porous ceramic compacts. It is noted that the dominant path for diffusion is usually along the grain boundary. Classical grain-boundary diffusion mechanism assumes that grain boundaries act as perfect sources and sinks for the diffusing atoms during the diffusion process and the energy provided is all available to drive the diffusional flux along the grain boundaries. The low GBD activation energy (compared with VD) is because the grain boundary is more active and it serves as a tunnel for diffusion.

The results given in figure 5, covering a wide range of densities and temperatures, show a decline in activation energy at high relative densities and temperatures. The same phenomena can be found in the literature (Liu *et al* 2001; Guillaume and Christian 2007). It is suggested that more than one densification mechanism is operative in the sintering experiments. Considering the decreasing activation energy trend in the present results, it is reasonable to deduce that the VD is the dominant densification mechanism for the α-Al_2O_3 powder at low relative density. At the beginning of sintering, the atom diffusion was difficult as a result of the long distance among particles in the samples. So, the apparent value of Q reflects this difficulty by having a high value. When the specimen densified further, more grain boundaries are formed, grain boundary diffusion will contribute to the densification of the specimen and Q becomes less.

4. Conclusions

Sintering in air of a granulated commercially-available alumina powder has been investigated by the way of a push rod type dilatometer tests. Based on the Arrhenius theory, it is found that the value of apparent activation energy for the mechanism controlling densification, Q, is a strong function of the relative density. The apparent activation energy decreases with the increase of the relative density. In addition, the value of the evaluated activation energy is different at the same density level when the Arrhenius plot involves different heating rates. It can be attributed to the difference of the relative contribution of D_l and D_b to the densification rate.

Acknowledgement

This work was supported by Qingdao Nature Science Foundation No. 05-1-JC-89, P.R. China

References

Coble R L 1961 *J. Appl. Phys.* **32** 787
Ewsuk K G, Ellerby D T and DiAntonio C B 2006 *J. Am. Ceram. Soc.* **89** 2003
Fang T T, Shive J T and Shiau F S 2003 *Mater. Chem. Phys.* **80** 108
Guillaume B G and Christian G 2007 *J. Am. Ceram. Soc.* **90** 1246
Kuczynski G C 1949 *Trans. Am. Inst. Mining. Met. Eng.* **185** 169
Kutty T R G, Khan K B, Hegde P V, Sengupta A K, Majumdar S and Purushotham D S C 2001 *J. Nucl. Mater.* **297** 120
Kutty T R G *et al* 2002 *J. Nucl. Mater.* **305** 159
Lahiri D, Ramana Rao S V, Hemantha Rao G V S and Srivastava R K 2006 *J. Nucl. Mater.* **357** 88
Liu Z Y, Loh N H, Khor K A and Tor S B 2001 *Scr. Mater.* **44** 1131
Matsui K, Ohmichi N and Ohgai M 2005 *J. Am. Ceram. Soc.* **88** 3346
McCoy J K and Wills R R 1987 *Acta Metall.* **35** 577
Sato E and Carry C P 1996 *J. Am. Ceram. Soc.* **79** 2156
Su H and Johnson D L 1996 *J. Am. Ceram. Soc.* **79** 3211
Tatami J, Suzuki Y, Wakihara T, Meguro T and Komeya K 2006 *Key Eng. Mater.* **317–318** 11
Wang J and Raj R 1990 *J. Am. Ceram. Soc.* **73** 1172
Wang J and Raj R 1991 *J. Am. Ceram. Soc.* **74** 1959
Young W S and Cutler I B 1970 *J. Am. Ceram. Soc.* **53** 659